Defence Science Journal, Vol. 57, No. 1, January 2007, pp. 69-77

Characterisation of Piezoelectric Ceramics

D.D. Ebenezer

Naval Physical and Oceanographic Laboratory, Kochi-682 021

ABSTRACT

The IEEE standard on piezoelectricity recommends methods to determine the coefficients of piezoelectric ceramics and the sizes of the samples to be used. A method to determine the difference between the actual coefficients and the coefficients determined using the IEEE standard is presented. The difference or error for samples of various shapes and sizes is presented. These errors and manufacturing considerations are used to make recommendations of the actual sizes of piezoceramics in various shapes to be used for material characterisation. Often, the IEEE standard cannot be used to determine the coefficients of piezoceramics used in underwater transducers and other devices because of their shapes and sizes. Radially polarised tubes and axially polarised rings used in hydrophones and projectors, respectively, are the examples. A method to determine some of the complex coefficients of tubes used for quality control during production is presented. Finally, an analytical model that can be used to develop a similar method for rings is presented. Several numerical results are presented to illustrate the methods.

Keywords: Piezoelectric, polymeric materials, PVDF, hydrophones, acoustic signal, pressure-release system, ceramics, piezoelectric ceramics

1. INTRODUCTION

Developers as well as users of new materials of new materials are interested in the characterisation of piezoelectric ceramics. The former are interested in all the ten coefficients[1] that define a material and use material samples whose sizes satisfy the recommendations, for characterisation, in the IEEE standard on piezoelectricity[2].

The latter are more interested in characterising the piezoceramics used in devices and the sizes of these usually violate the recommendations in the IEEE standard. In this paper, characterisation of some samples that satisfy and others that do not satisfy the IEEE recommendations is presented in brief.

2. ERRORS IN CHARACTERISATION USING STANDARD EQUATIONS

The standard recommendations for the sizes of slabs and rods used for characterisation are $L>>W$ and $L>>t$. Here, L, W and t are the length, width, and thickness, respectively. These qualitative requirements become more stringent as the piezoelectric coupling increases[2]. The electrode area is $L \times W$ and $W \times t$ for slabs and rods, respectively are shown in Fig. 1. For slabs, $W > 3t$ is also recommended. For discs, shown in Fig. 1, the recommendation is, $a > 20\ t$ for finding s_{11}^E and $a > 40\ t$ for finding, s_{12}^E where a and t are the radius and distance between electrodes, respectively. Slabs are used to find ε_{33}^T, s_{11}^E and d_{31}; rods are used to find ε_{33}^T,

Revised 16 September 2006

S_{33}^D and d_{33}; and discs are used to find ε_{33}^T, s_{11}^E, s_{12}^E and d_{31}. The coefficients are also used to find the piezoelectric coupling coefficient k_{31} in slabs and discs and k_{33} in rods.

The errors[3] in the coefficients determined using the standard equations are determined as follows: The input electrical admittances of piezoelectric slabs, rods, and discs, of various sizes, are first computed using a set of 10 piezoelectric coefficients and the 3-D finite element program ATILA[4] as shown in Fig. 2. It is possible, in principle, to solve the inverse problem, i.e., use the computed input electrical admittance to determine the 10 coefficients input to ATILA. If this is done exactly, the set of coefficients input to ATILA can be recovered exactly. However, this is not easy as some of the coefficients have very little effect on the admittance when the dimensions of the slab, rod or disc satisfy the recommendations in the Standard. The 10 piezoelectric coefficients of PZT4 input to ATILA are s_{11}^E = 12.3 x 10^{-12} m^2/N, s_{12}^E = -4.05 x 10^{-12} m^2/N, s_{13}^E = -5.31 x 10^{-12} m^2/N, s_{33}^E=15.5 x10^{-12} m^2/N, s_{44}^E=39x10^{-12} m^2/N, d_{31}= -123 x 10^{-12} C/N, d_{33}=289x10^{-12} C/N, d_{15}= 496 x 10^{-12} C/N, ε_{11}^S, and ε_{33}^S. The values of ε_{11}^S and ε_{33}^S are computed using the values of the other eight coefficients, $\varepsilon_{11}^T / \varepsilon_0$ =1475, and $\varepsilon_{33}^T / \varepsilon_0$ =1300. The coefficients in the set input to ATILA, and those calculated using the relationships[2] between different sets, are the actual values.

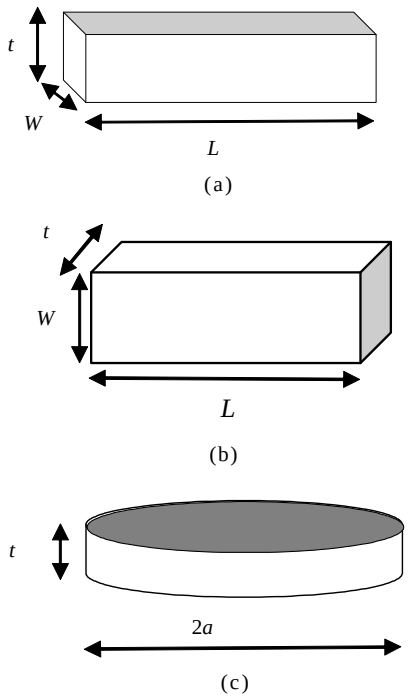

Figure 1. (a) A length expander slab with perpendicular field. Sides with area *LxW* are fully electroded, (b) A length expander rod with parallel field. Sides with area *Wxt* are fully electroded, (c) A disc of radius *a* and thickness *t*. The flat surfaces are fully electroded.

The computed admittances and the approximate 1-D standard equations are then used to calculate some piezoelectric coefficients. The difference between the actual coefficient and that obtained using the standard equations is the error for that particular case. Errors exist because the standard equations are based on 1-D models. Normally, measured values are used in place of the computed admittances and the actual coefficients are not known and the error cannot be determined.

Results of the computations are given here for each of the 3 shapes considered in this study. The piezoelectric coefficients determined for slabs, rods and discs are shown in Tables 1, 2, and 3 respectively. The "actual values" in the last row of each table are those in the set input to ATILA or computed from that set. It is of interest to note that the percentage error in the coupling coefficient is often less than the percentage error in the corresponding S^E, S^D or d coefficient. It is also seen that the error is not very large even when the sizes of the samples are similar to those used in piezoelectric devices and do not conform to the standard recommendations. In most cases, d_{31} of slabs is underestimated by a few per cent, d_{33} of rods is overestimated by a few per cent, and d_{31} of thin discs is nearly accurate. This is of interest to developers of new materials and also to transducer designers.

3. CHARACTERISATION OF RADIALLY POLARISED TUBES

Radially polarised piezoelectric ceramic tubes are widely used in hydrophones. It is difficult to control their properties from one batch to the next and this can cause variations in the characteristics of hydrophones. One approach to reduce rejection of costly tubes as well as large variations in the

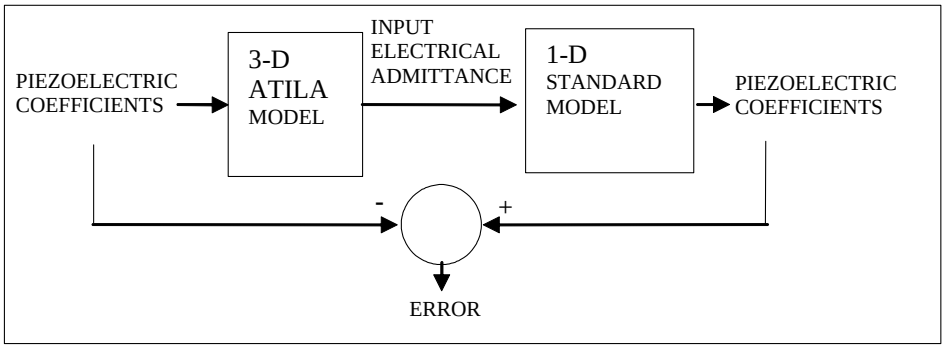

Figure 2. Flow chart for finding errors.

Table 1. Coefficients of slabs obtained using standard equations

L **(mm)**	***W*** **(mm)**	***t*** **(mm)**	$\varepsilon_{33}^T/\varepsilon_0$	s_{11}^E **(pm²/N)**	***d*₃₁ (pC/N)**	***k*₃₁**
100	30	10	1.30e3	12.4	-119	-0.310
100	25	10	1.30e3	12.4	-120	-0.320
100	12	5	1.30e3	12.3	-123	-0.330
40	20	5	1.30e3	12.7	-108	-0.280
40	10	5	1.30e3	12.4	-121	-0.320
40	10	3	1.30e3	12.4	-120	-0.320
40	8	3	1.30e3	12.4	-121	-0.320
Actual values			1.30e3	12.3	-123	-0.327

Table 2. Coefficients of rods obtained using standard equations

L **(mm)**	***W*** **(mm)**	***t*** **(mm)**	$\varepsilon_{33}^T/\varepsilon_0$	s_{33}^D **(pm²/N)**	***d*₃₃ (pC/N)**	***k*₃₃**
10	2	2	1.30e3	8.28	291	0.690
10	3	3	1.30e3	8.34	293	0.690
10	4	4	1.30e3	8.43	296	0.690
10	5	5	1.30e3	8.55	300	0.690
Actual values			1.30e3	8.24	289	0.684

Table 3. Coefficients of dics obtained using standard equations

a **(mm)**	***t*** **(mm)**	$\varepsilon_{33}^T/\varepsilon_0$	s_{11}^E **(pm²/N)**	s_{12}^E **(pm²/N)**	***d*₃₁ (pC/N)**	***k*₃₁**
10	1	1.30e3	12.6	-4.36	-123	-0.320
10	2	1.30e3	13.8	-5.55	-124	-0.310
30	1	1.30e3	12.3	-4.08	-123	-0.330
40	1	1.30e3	12.3	-4.07	-123	-0.330
60	1	1.30e3	12.3	-4.08	-123	-0.330
25	4	1.30e3	18.4	-10.3	-127	-0.280
Actual values		1.30e3	12.3	-4.05	-123	-0.327

characteristics of hydrophones is to bin the tubes based on their material properties–particularly those that affect hydrophone performance. Piezoelectric coefficients determined for this application are likely to have higher errors because the tubes are not slender. Nevertheless, the results are useful if the variation in hydrophone characteristics is reduced.

Ebenezer and Sujatha[5] presented methods to determine the coefficients ε_{33}^T, s_{11}^E, s_{12}^E, and d_{31} of radially polarised piezoelectric tubes as shown in Fig. 3. They used the membrane model. Later, Ebenezer[6] determined the complex coefficients using thin shell theory and a method (briefly described here). The method can be used for both: characterisation of new materials and components for devices. In this method, the value of ε_{33}^T is first determined

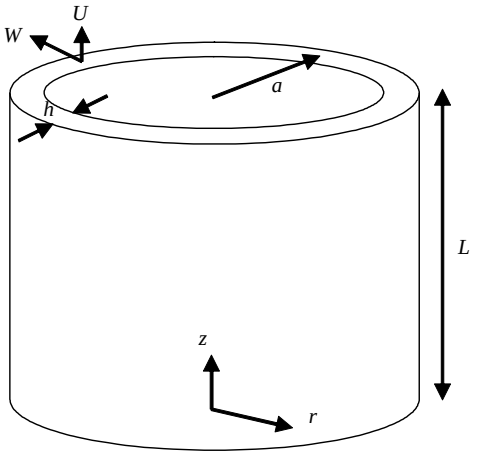

Figure. 3. A thin radially polarized cylindrical tube of length *L* and radius *a*. The inner and outer curved surfaces are fully electroded.

using the measured complex admittance, *Y*, at a frequency much lower than the lowest resonance frequency. Alternatively, if dispersion is significant, it is measured at a few low frequencies and its value at higher frequencies is determined by extrapolation. The real and imaginary parts of s_{11}^E, s_{12}^E, and d_{31} are then determined by iteratively refining them until the measured values of six functions are nearly equal to those computed using the analytical model[7] and the refined coefficients.

The six functions used to determine the piezoelectric coefficients are all frequencies. These are the frequencies f_s^L and f_s^U in the lower and upper branches, respectively, at which the conductance, *G*, reaches a local maximum; the frequency f_p^U in the upper branch at which the resistance, *R*, reaches a local maximum; and the three bandwidths $f_{1/2s}^L - f_{-1/2s}^L$, $f_{1/2s}^U - f_{-1/2s}^U$, and $f_{1/2p}^U - f_{-1/2p}^U$ where $f_{1/2s}^L$ and $f_{-1/2s}^L$ are the frequencies in the lower branch at which *B* reaches a local minimum and maximum, respectively, and are the frequencies in the upper branch at which *B* reaches a local minimum and maximum, respectively, and $f_{1/2p}^U$ and $f_{-1/2p}^U$ are the frequencies in the upper branch at which the reactance, *X*, reaches a local minimum and maximum, respectively.

Then, an initial guess is made for the six unknowns –real and imaginary parts of s_{11}^E, s_{12}^E, and d_{31}. The real parts of the initial guess are values obtained using 'book values' and the imaginary parts are small, non-zero, and satisfy the conditions in Ref. 8. In the first step of iteration of the first cycle, the guesses for Re(s_{11}^E) and Re(s_{12}^E) are refined using the measured frequencies f_s^L and f_s^U, and

$$\begin{Bmatrix} \hat{x}_1 \\ \cdots \\ \hat{x}_N \end{Bmatrix} = \begin{Bmatrix} \overline{x}_1 \\ \cdots \\ \overline{x}_N \end{Bmatrix} + \begin{bmatrix} \frac{\partial f_1}{\partial x_1} & \cdots & \frac{\partial f_1}{\partial x_N} \\ \cdots & \cdots & \cdots \\ \frac{\partial f_N}{\partial x_1} & \cdots & \frac{\partial f_N}{\partial x_N} \end{bmatrix}^{-1} \begin{Bmatrix} f_1^M - f_1 \\ \cdots \\ f_N^M - f_N \end{Bmatrix} \quad (1)$$

where x_i, $\overline{x_i}$, $\hat{x}_i$, f_i, f_i^M, i = 1, 2, …*N*, are the unknowns, the initial guesses, the refined guesses at the end of the current step, functions whose values are measured, and measured values of the functions, respectively, and *N* = 2. The partial derivatives and are evaluated using the analytical model at $\overline{x_i}$, i = 1, 2, …*N* and $\overline{y_j}$, *j* = *N*+1, *N*+2 …6 where $\overline{y_j}$ are the guessed values of the unknowns that are not refined in the current step of the iteration. Equation (1) is based on a Taylor series expansion for each function in terms of the piezoelectric coefficients and the Newton-Raphson method.

In the second step of the cycle, the value of Re(d_{31}) is refined using f_p^U and Eqn (1) with *N* = 1. In the third step, the values of Im(s_{11}^E), Im(s_{12}^E), and Im(d_{31}) are simultaneously refined using the three bandwidths and Eqn (1) with *N* = 3. Each step is done twice before proceeding to the next step. The three steps together constitute one cycle. The entire cycle is repeated twice or thrice or until some prescribed convergence is obtained.

Numerical results are presented to illustrate the robustness and accuracy of the iteration method. All calculations are done using the four sets of dimensions shown in Table 4 that are representative of those used in hydrophones. Sets of the four complex coefficients and determined by iteration are shown in Table 5(a). These, together with the six coefficients shown in Table 5(b), form a set of 10 coefficients necessary to completely describe piezoelectric materials. The density is 7750 kg/m^3. The functions that are usually measured are calculated using the coefficients in Table 5(b), any one set from Table 5(a), and the finite element model ATILA.

Table 4. Dimensions of radially polarised cylindrical tubes

Dimension	*L* (mm)	*a* (mm)	*t* (mm)
A	20	15	1
B	10	10	1
C	20	15	3
D	10	10	2

Table 5(a). Piezoelectric coefficients input to ATILA and determined by iteration

Case	$\varepsilon_{33}^T / \varepsilon_0$	s_{11}^E (pm²/N)	s_{12}^E (pm²/N)	d_{31} (pC/N)
a	1700(1-j0.02)	16.4-j0.30	-5.74+j0.10	-171+j3.0
b	1700(1-j0.02)	15.5-j0.80	-6.50+j0.50	-150+j1.0
c	1700(1-j0.02)	17.5-j0.80	-6.50+j0.50	-150+j1.0
d	1700(1-j0.02)	15.5-j0.80	-6.50+j0.50	-190+j1.0
e	1700(1-j0.02)	16.4-j0.30	-5.74+j1.0	-166+j3.0

Table 5(b). Additional piezoelectric coefficients input to ATILA

$\varepsilon_{11}^T / \varepsilon_0$	s_{33}^E (pm²/N)	s_{13}^E (pm²/N)	s_{44}^E (pm²/N)	d_{31} (pC/N)	d_{31} (pC/N)
1730 (1-j0.02)	18.8-j0.30	-7.22+j0.15	47.5-j1	374-j7	584-j10

Critical frequencies are computed using ATILA with a resolution of 10 Hz and input to the iteration procedure. The low resolution is used to account for measurement errors that may occur. For example, the values in kHz of $f_{1/2s}^L$, f_s^L, $f_{-1/2s}^L$, $f_{1/2s}^U$, f_s^U, $f_{-1/2s}^U$, $f_{1/2p}^U$, f_p^U, and $f_{-1/2p}^U$ for dimension **A**, Case *a* are 29.17, 29.44, 29.70, 75.09, 75.80, 76.50, 86.34, 87.20, and 88.08, respectively. The refined coefficients obtained from the iteration procedure are shown in Table 6, after rounding-off, for the various dimensions and cases shown in Tables 4 and 5, respectively.

The initial guess for the four complex coefficients is the same in all cases and is shown in row *a* of Table 5(a). It is seen from Table 5(a) that both the real and imaginary parts of the coefficients in the other rows differ considerably from row *a*. This indicates that the method is not sensitive to the initial guess.

It is seen from Table 6 that the error increases when the ratio of wall thickness to radius or wall thickness to length increases. The error in the real parts of the coefficients is minimum for s_{11}^E, slightly greater for d_{31}, and greatest for s_{12}^E. $\mathrm{Re}(s_{11}^E)$ and $|\mathrm{Re}(s_{12}^E)|$ are underestimated, and $|\mathrm{Re}(d_{31})|$ is overestimated. $|\mathrm{Im}(s_{11}^E)|$ and $\mathrm{Im}(s_{12}^E)$ are overestimated except for case *e* where $\mathrm{Im}(s_{12}^E)$ is underestimated, and $\mathrm{Im}(d_{31})$ is sometimes overestimated and sometimes underestimated.

Table 6. Coefficients obtained by iteration for dimensions and coefficients shown in Table 1 & 2 respectively

Dimension	Case	s_{11}^E (pm²/N)	s_{12}^E (pm²/N)	d_{31} (pC/N)
A	a	16.4-j0.30	-5.72+j0.095	-171+j3.0
	b	15.5-j0.80	-6.48+j0.50	-150+j0.98
	c	17.5-j0.81	-6.48+j0.51	-150+j0.98
	d	15.5-j0.80	-6.49+j0.50	-190+j1.0
B	a	16.4-j0.30	-5.64-j0.097	-172+j3.0
	b	15.5-j0.80	-6.40+j0.50	-151+j1.0
	c	17.5-j0.80	-6.41+j0.50	-151+j0.98
	d	15.5-j0.80	-6.40+j0.50	-191+j0.95
C	a	16.3-j0.30	-5.47+j0.095	-173+j3.1
	b	15.4-j0.80	-6.26+j0.50	-152+j0.97
	c	17.4-j0.80	-6.25+j0.50	-152+j0.98
	d	15.4-j0.80	-6.26+j0.50	-192+j0.98
	e	16.3-j0.30	-5.47+j0.097	-168+j3.0
D	a	16.3-j0.30	-5.30+j0.089	-176+j3.1
	b	15.4-j0.79	-6.07+j0.50	-155+j0.95
	c	17.4-j0.79	-6.08+j0.50	-155+j0.99
	d	15.4-j0.80	-6.07+j0.50	-194-j0.96
	e	16.3-j0.30	-5.30+j0.090	-171+j3.1

The value of g_{31} has a strong influence on the receiving sensitivity of radially polarised cylindrical tube. Here, the percentage error in $\mathrm{Re}(g_{31})$ is equal to the percentage error in $\mathrm{Re}(d_{31})$ because $g_{31} = d_{31}/\varepsilon_{33}^T$ and it is assumed that ε_{33}^T is exactly determined. For Dimension A, there is no error to three significant digits in $\mathrm{Re}(g_{31})$ as seen from Table 3. For the other dimensions and cases, $|\mathrm{Re}(g_{31})|$ is consistently overestimated by a small amount. Therefore, it is concluded that the iteration procedure can be used to estimate $\mathrm{Re}(g_{31})$ and bin tubes produced in large numbers according to their properties.

4. CHARACTERISATION OF AXIALLY POLARISED RINGS

Consider an axially polarised piezoelectric ceramic ring of length *L*, inner and outer radii *a* and *b*,

respectively as shown in Fig.4. The inner radius is a few-time the wall thickness, which is nearly the same as the length. The top and bottom surfaces are fully electroded and a known voltage is applied between these. The input electrical admittance and a few characteristic frequencies are of interest.

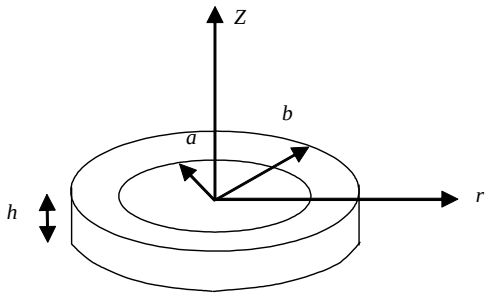

Figure. 4. A piezoceramic ring with electrodes on the flat surfaces.

Ebenezer[9-11], *et al*. analysed axially polarised solid cylinders. They assumed[9] that the axial displacement and potential are functions of only the axial coordinate and that the radial displacement is a function of only the radial coordinate. They showed[9] that, for example, the analysis is exact when shear stress is zero on all the surfaces and the normal displacements are specified on the surfaces.

They extended the model to analyse rings with free boundary conditions[12]. An exact solution to the governing equations is written as

$$\begin{Bmatrix} U \\ W \\ \phi \end{Bmatrix} = \begin{Bmatrix} A\sin(k_z z) \\ BJ_1(k_r r) + QY_1(k_r r) \\ A(e_{33}/\varepsilon_{33}^S)\sin(k_z z) \end{Bmatrix} \quad (2)$$

where, U and W are the axial and radial components of displacement respectively, ϕ is the electric potential, $k_r = \omega\sqrt{\rho / c_{11}^E}$, $c_{33}^D = c_{33}^E + e_{33}^2 / \varepsilon_{33}^S$ and $k_r = \omega\sqrt{\rho / c_{11}^E}$, and J_1 and Y_1 are the first-order Bessel functions of the first and second kind, respectively.

The input electrical admittance of piezoceramic rings is calculated after using the boundary conditions to determine the coefficients in Eqn. (2). Material losses are accounted for using complex coefficients shown in Table 7. The real parts of these coefficients are obtained using certain coefficients for Navy type I piezoceramics.

Table 7. Material parameters of piezoceramic used in the model

Property	Value
c_{11}^E (GNm^{-2})	138.995 + j 0.695
c_{12}^E (GNm^{-2})	77.835 + j 0.389
c_{13}^E (GNm^{-2})	74.282 + j 0.371
c_{33}^E (GNm^{-2})	115.409 + 0.577
e_{31} (Cm^{-2})	-5.203
e_{33} (Cm^{-2})	15.080
ρ (kgm^{-3})	7500
ε_{33}^S (pFm^{-1})	5.872 - j 0.018

The parameters computed and shown in Table 8 are the lowest frequency, f_s, at which the conductance G is maximum; the maximum value of G; the frequency, $f_{1/2s}$, at which the susceptance B is locally maximum; the maximum value of B; the frequency, $f_{-1/2s}$, at which B is locally minimum; the minimum value of B; and the frequency f_a at which B is zero. All the computations are done for both the lower and the upper branches but the upper branch is of more interest for transducer designers. Results are shown for rings with various dimensions and are compared with those obtained using the Flugge model[13] and ATILA.

It is seen from Table 8 that the values computed using the present model are closer to the values computed using ATILA in most cases than those computed using the Flugge model. In cases *A*, *B*, and *C*, the length is equal to or greater than the wall thickness and all the frequencies computed using the present model, except f_a in the upper branch for case *B*, are closer to ATILA values. In cases *C* and *D*, wall thickness is equal to length and the present model is always better. In cases *A*, *B*, and *F*, length is less than twice the wall thickness and the maximum and minimum values of *G* and *B* in the upper branch computed using the Flugge model are closer to ATILA values. In

Table 8. Computed parameters for piezoelectric rings with internal losses.

	Dimension 2b, 2a, L, b-a (mm)	Branch	Model	f_s (kHz) and ε_{max} (mS)	$f_{1/2s}$ (kHz) and B_{max} (mS)	$f_{-1/2s}$ (kHz) and B_{min} (mS)	f_a (kHz)
A	50, 38, 8, 6	Lower	Present	23.99 (3.99)	23.93 (2.16)	24.05 (-1.85)	25.44
			ATILA	23.96 (3.98)	23.90 (2.15)	24.02 (-1.84)	25.41
			Flugge	23.87 (3.87)	23.81 (2.09)	23.93 (-1.78)	25.27
		Upper	Present	192.2 (102)	191.7 (51.4)	192.7 (-50.1)	246.9
			ATILA	189.4 (95.9)	188.9 (48.6)	189.9 (-47.3)	236.0
			Flugge	205.4 (98.8)	204.9 (50.2)	205.9 (-48.6)	254.4
B	50, 38, 10, 6	Lower	Present	23.97 (3.24)	23.91 (1.74)	24.03 (-1.49)	25.43
			ATILA	23.95 (3.22)	23.89 (1.74)	24.01 (-1.49)	25.40
			Flugge	23.85 (3.12)	23.79 (1.69)	23.91 (-1.44)	25.26
		Upper	Present	159.3 (66.4)	159.0 (33.6)	159.7 (-32.8)	203.6
			ATILA	157.5 (64.1)	157.1 (32.5)	157.9 (-31.6)	198.5
			Flugge	163.6 (60.1)	163.2 (30.6)	164.0 (-29.5)	193.5
C	50, 38, 6, 6	Lower	Present	24.00 (5.30)	23.94 (2.86)	24.06 (-2.44)	25.44
			ATILA	23.97 (5.26)	23.91 (2.84)	24.03 (-2.43)	25.41
			Flugge	23.88 (5.12)	23.82 (2.77)	23.94 (-2.35)	25.27
		Upper	Present	234.6 (159.5)	234.0 (80.9)	235.2 (-78.6)	296.9
			ATILA	228.7 (136.8)	228.1 (69.7)	229.2 (-67.1)	267.5
			Flugge	274.3 (178.1)	273.6 (90.4)	275.0 (-87.7)	341.7
D	50, 34, 8, 8	Lower	Present	25.32 (5.53)	25.26 (2.97)	25.38 (-2.55)	26.89
			ATILA	25.27 (5.49)	25.21 (2.95)	25.33 (-2.53)	26.83
			Flugge	25.08 (5.15)	25.01 (2.78)	25.14 (-2.37)	26.54
		Upper	Present	176.7 (113)	176.3 (57.5)	177.0 (-52.2)	223.2
			ATILA	172.2 (96.5)	171.8 (49.1)	172.7 (-47.3)	201.1
			Flugge	204.9 (125)	204.4 (63.6)	205.4 (-61.6)	254.3
E	50, 42, 8, 4	Lower	Present	22.84 (2.61)	22.78 (1.41)	22.89 (-1.20)	24.19
			ATILA	22.83 (2.60)	22.77 (1.40)	22.88 (-1.20)	24.18
			Flugge	22.79 (2.58)	22.73 (1.39)	22.85 (-1.19)	24.13
		Upper	Present	202.2 (73.1)	201.6 (37.2)	202.7 (-36.1)	251.5
			ATILA	200.0 (71.0)	199.5 (36.0)	200.5 (-35.0)	252.2
			Flugge	202.0 (42.9)	201.5 (23.0)	202.5 (-19.7)	209.2
F	40, 28, 8, 6	Lower	Present	31.19 (4.14)	31.11 (2.23)	31.26 (-1.92)	33.12
			ATILA	31.14 (4.12)	31.06 (2.22)	31.21 (-1.91)	33.06
			Flugge	30.93 (3.91)	30.85 (2.11)	31.01 (-1.80)	32.75
		Upper	Present	192.8 (77.9)	192.3 (39.5)	193.2 (-38.5)	247.2
			ATILA	189.9 (73.5)	189.5 (37.3)	190.4 (-36.2)	236.4
			Flugge	204.7 (74.7)	204.2 (37.9)	205.2 (-36.7)	251.9

case E, the length is twice the wall thickness and the upper branch resonance frequencies computed using the Flugge model are a little closer to ATILA values. The good agreement indicates that the analytical model and the measured values of the parameters shown in Table 8 can be used to determine the piezoelectric coefficients of axially polarised rings.

5. CONCLUSION

Methods to characterise slabs, bars, discs, radially polarised tubes, and axially polarised rings have been summarised. The errors in determining the real coefficients of slabs, bars, discs using the IEEE standard method are quantified for various dimensions. Based on these, it is recommended that slabs of size 100 x 12 x 5 mm and rods of size 10 x 2 x 2 mm be used for characterisation. For discs, even though the IEE Standard recommends a > 40 *t* for finding s_{12}^{E}, it is seen that the results are quite accurate for some applications even for smaller radius to thickness ratios. However, discs of size 40 x 1 mm can be precisely made and used for characterisation. An iterative method, that can be used if a fairly accurate analytical model is available, is also presented. It is illustrated by finding the complex coefficients of radially polarised tubes. The analytical model is based on thin shell theory and is therefore fairly accurate even when the wall thickness to radius ratio is not very small as is often the case in tubes used in hydrophones.

An analytical model of piezoelectric rings is also presented and numerical results are presented to illustrate the accuracy of the model. The iterative method used to determine the coefficients of radially polarised tubes can be used to determine the coefficients of axially polarised rings also.

Certain assumptions are made in the analytical standard models and in the models developed by Ebenezer[10], *et al*. and co-workers. These approximate models are used to solve the inverse problem though the forward problem is solved exactly using the finite element method. The errors arise because of the approximations made in the analytical models. More numerical results are presented by Ebenezer,[3,6] *et al*.

ACKNOWLEDGMENTS

Permission from Shri V. Chander, Director, Naval Physical and Oceanographic Laboratory, KOchito publish this paper, is gratefully acknowledged.

REFERENCES

1. Sherrit, S.; Wiederick, H.D.; & Mukherjee, B.K. A complete characterisation of the piezoelectric, dielectric, and elastic properties of Motorola PZT 3203 HD including losses and dispersion. *In* Ultrasonic Transducer Engineering: Proceedings SPIE 3037, SPIE, Bellingham, WA 98227, USA, 1997. pp. 158-69.

2. IEEE Standard on Piezoelectricity, ANSI/IEEE Standard. 176-1987. IEEE *Trans. Ultrasonics Ferroelect. Freq. Cont*., 1996, *UFFC*-**43**, 717-72.

3. Ebenezer, D.D. & Sujatha, A.J. Errors in the characterisation of piezoelectric ceramics. *In* Proceedings of ISSS-SPIE International Conference on Smart Materials, Structures and Systems, Bangalore, 2002. pp. 131-38.

4. ATILA Users Manual, Version 5.2.4.

5. Ebenezer, D.D. & Sujatha, A.J. New methods to characterise radially polarised piezoelectric ceramic cylindrical shells of finite length. *J. Acoust. Soc. Am.*, 1997, **102**(3), 1540-548.

6. Ebenezer, D.D. Determination of complex coefficients of radially polarized piezoelectric ceramic cylindrical shells using thin shell theory. *IEEE Trans. Ultrasonics Ferroelect. Freq. Cont*., 2004, **51**(10), 1209-215.

7. Ebenezer, D.D. & Abraham, P. Closed-form analysis of thin radially polarised piezoelectric ceramic cylindrical shells with loss. *Current Science*, 2002, **83**(8), 981-88.

8. Holland, R. Measurement of piezoelectric phase angles in a ferroelectric ceramic. *IEEE Trans. Sonics Ultrasonics*, 1970, **SU-17**(2), 123-24.

9. Ebenezer, D.D. & Ramesh, R. Exact analytical model of axially polarised piezoceramic cylinders with certain uniform boundary conditions. *Current Science*, 2003, **85**(8), 1173-179.

10. Ebenezer, D.D. & Ramesh, R. Analysis of axially polarised piezoceramic cylinders with arbitrary boundary conditions on the flat surfaces. *J. Acoust. Soc. Am.*, 2003, **113**(4), 1900-908.

11. Ebenezer, D.D.; Ravichandran, K.; Ramesh, R. & Padmanaban, C. Forced responses of solid axially polarised piezoelectric ceramic finite cylinders with internal losses. *J. Acoust. Soc. Am.*, 2005, **117**(7), 3645-656.

12. Ramesh, R. & Ebenezer, D.D. Analysis of axially polarised piezoceramic rings. *Ferroelectrics* 2005, **323**, 17-23.

13. Ebenezer, D.D. & Abraham, P. Analysis of axially polarised piezoelectric ceramic cylindrical shells of finite length with internal losses. *J. Acoust. Soc. Am.*, 2002, **112**(5), 1953-960.

Contributor

Dr D.D. Ebenezer obtained his BTech (Naval Architecture) from the Indian Institute of Technology Madras, Chennai, and PhD (Ocean Engg) from the University of Rhode Island, USA, 1990. Since 1990, he has been working in the Naval Physical and Oceanographic Laboratory (NPOL), Kochi, where he is currently the Head of the Transducer Group. His present research interests include: Modelling of piezoceramics and underwater transducer systems. He has published 20 papers in international peer reviewed journals. He received *DRDO Technology Day Award* (2002), and the *DRDO Science Day Commendation* (2005).